Ecological Engineering 135 (2019) 36–44

Contents lists available at ScienceDirect

Ecological Engineering

journal homepage: www.elsevier.com/locate/ecoleng

Impact of sand mining on alluvial channel flow characteristics

Bandita Barman[a,b], Bimlesh Kumar[c,*], Arup Kumar Sarma[c]

[a] State Key Laboratory of Water Resources and Hydropower Engineering Science, Wuhan University, China
[b] Indian Institute of Technology Guwahati, India
[c] Department of Civil Engineering, Indian Institute of Technology Guwahati, Guwahati 781039, India

ARTICLE INFO

Keywords:
Mining pit
Turbulent parameters
Bursting events

ABSTRACT

Mining pit in a channel bed causes disturbance to the flow characteristics. To interpret the phenomenon of change in flow characteristics in a mining pit, experimental study was performed in a tilting laboratory flume. This research focuses on the impact of mining pit on different turbulent parameters, such as flow velocity, Reynolds shear stress distribution, turbulent kinetic energy fluxes, and higher order moment distribution. We have observed dropped in flow velocity in the pit and also significant reversal velocity layer at the pit bottom. The analysis of Reynolds shear stress and higher order moment distribution shows higher values of velocity fluctuations in the pit than the upstream section. The response of bursting events, which is identified by the third order moment, shows influence of sweep events near the bed in all four sections. Third order moment analysis also shows a rise in dominance of sweep events along the flow depth in the pit and it's downstream, compared to the upstream section. The kurtosis distribution shows highly intermittent nature of turbulence close to the channel bed. The longitudinal turbulent kinetic energy fluxes and vertical turbulent kinetic energy fluxes are in downstream and downward directions for both inner and outer layer in the pit region, which shows an increase in bed particle mobility in that region, whereas it is present only in the inner layer at the upstream section. Additionally, improved bed load transport equation by incorporating pit geometry has been proposed for alluvial channel subjected to sand mining.

1. Introduction

River beds are seldom free of disturbance causes by human being. Sand mining is considered as such disturbance that increases the interaction of sediment with flow and changes the river morphology. The turbulent nature of flows in stream and canal causes bedload transport. Although the impact of sand mining on channel morphology has been studied for decades (Collins and Dunne, 1989; Rinaldi et al., 2005; Zawiejska et al., 2015), the hydrodynamic behavior of mining affected alluvial channel is still challenging due to the complex interaction between the flow and the mobile bed. The interaction of sediment and flow due to the continuous extraction of sand also causes an increase in turbidity of the river water (Erskine, 1990; Kim, 2005). Researchers have done on experiments with mining pit in flume, on empirical approaches for the migration of pit and channel bed deformation (Barman et al., 2017; Lee et al., 1993; Neyshabouri et al., 2002) and on turbulent characterization of flow in a mining pit region (Barman et al., 2018a). Presence of sand mining has significant effects on morphological characteristics such as channel bed degradation, erosion of river bank and change in the plan form of a river (Collins and Dunne, 1990; Sear and Archer, 1998). Ramkumar et al. (2015) investigated on sediment mining, dynamics of river bar and sediment texture characteristics of the Kaveri river, South India and documented the deterioration of natural fluvial system because of intensive sand mining activity and damming in the upstream river reach. Brestolani et al. (2015) conducted investigation on change in morphology of the river caused by large scale mining of gravel in Orco River, situated in the Piemonte region by using CNR-IRPI experimental methodology based on multi-years LiDAR surveys realized in the years 2003, 2004, 2006, and 2007. The study by Brestolani et al. (2015) showed incision at pit upstream and downstream. Chanel incision at both upstream and downstream of mining zone was also reported by Chen and Liu (2009), Rinaldi et al. (2005), and Zawiejska et al. (2015). Calle et al. (2017) conducted a GIS-based investigation in the Rambla de la Viuda (eastern Spain) stream for assessment of morphosedimentary changes due to in-stream gravel mining and the quantification of river bed degradation was done by using LiDAR DTM and RTK-GPS (Real Time Kinematic) measurements. The geomorphological changes were identified by Calle et al. (2017) with the help of 13 sets of aerial photographs captured in between 1946 and 2012 and the erosion map indicated a continuous lowering of river

* Corresponding author.
E-mail addresses: bandita.barman@iitg.ac.in (B. Barman), bimk@iitg.ac.in (B. Kumar), aks@iitg.ac.in (A.K. Sarma).

https://doi.org/10.1016/j.ecoleng.2019.05.013
Received 6 November 2018; Received in revised form 5 May 2019; Accepted 15 May 2019
Available online 22 May 2019
0925-8574/

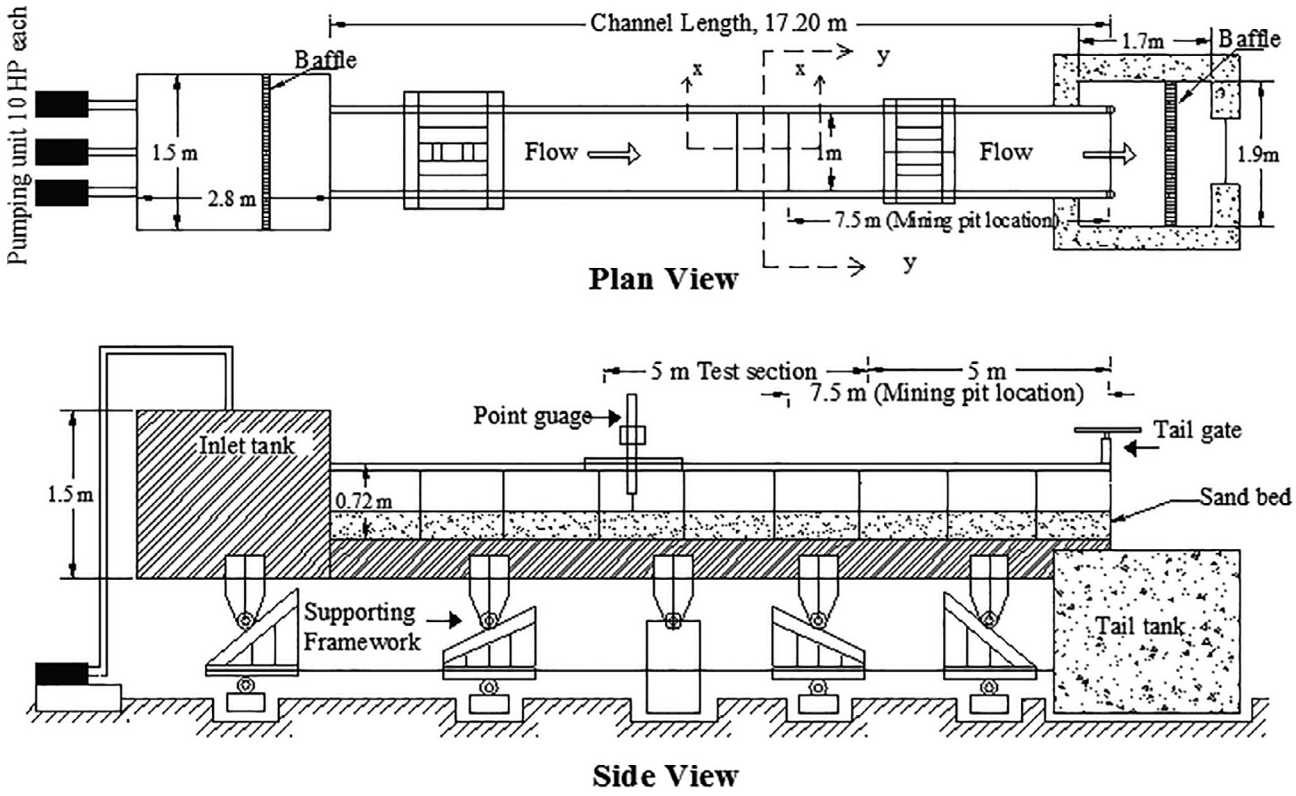

Fig. 1. Experimental setup.

bed since 1967 and observed degradation of almost 3.5 m at the time of study.

A great deal of previous studies has concentrated on the morphological impact of river aggregate mining and documented erosion of a river. For the evaluation of the morphological changes in a natural stream, it is essential to have a clear understanding on turbulent flow structures. Various researchers had work on to interpret the significance of turbulent flows and the mechanism of interaction of flow and sediment over the bed. The bursting phenomenon gave more understanding into the coherent structure of turbulent flows (Kline et al., 1967). Various bursting events such as ejections and sweeps generate near the bed region due to the occurrence of hairpin vortices (Best, 1992). Various researchers concentrated on turbulent structure of flow at threshold motion condition (Cao, 1997; Clifford et al., 1991; Dwivedi et al., 2010; Sutherland, 1967; Thorne et al., 1989). The characteristics of turbulent flows over an alluvial bed have also been studied by many researchers (Bennett and Bridge, 1995; Drake et al., 1988; Nelson et al., 1995; Nikora and Goring, 2000; Song and Graf, 1994; and Venditti et al., 2005). Sediment transport and mobile bed condition occur in the most of the natural alluvial stream because of interchange of momentum between the flow and the bed materials. The sediment mobility in a natural channel is highly influenced by the occurrence of disturbance on the stream bed. The channel bed morphology plays a deciding role in influencing the characteristics of the flow. Mining is a type of manmade disturbance that can influence the characteristics of turbulent structures in the flow. The long-term extraction of aggregates can cause some pit like structure in the river and can affect the local flow characteristics, which further changes the channel morphology (Yuill et al., 2016). Previously, the turbulent flow field in a trench was discussed by Alfrink and van Rijn (1983). Alfrink and van Rijn (1983) conducted an experiment in a trench having a layer of gravel and they measured instantaneous velocity by using a Laser Doppler Velocity. The experimental results from the study of Alfrink and van Rijn (1983) showed a reversal bottom velocity layer up to the center of the pit. A mining pit on a sand bed channel was used by Barman et al. (2018a) for investigating turbulent flow structures in the pit and found similar trend of result as that of Alfrink and van Rijn (1983). Barman et al. (2018a) also found considerably high intensities of velocity fluctuations and Reynolds shear stress in the mining pit region. In particular, a strong influence of sweep events in the pit region was observed in their study. Due to momentum exchange, a substantial portion of the flow momentum transfers into the bed material, and thus causes fluid energy dissipation. This phenomenon creates an enthusiasm to explore the exchange of energy and momentum in the mining pit region, in terms of turbulent kinetic energy fluxes. The turbulence created in the pit region can also be discussed through the determination of various higher order co-relations of velocity fluctuations. This research, therefore addresses mainly the higher order correlation of velocity fluctuation and turbulent kinetic energy fluxes in a mining pit region. It is also aimed to develop an improved bed load equation for sand mining affected alluvial channel incorporating the geometrical parameters.

2. Detailed experimental description

A recirculating, tilting laboratory flume was used to carry out the experiments. The flume has a length of 17.2 m, width 1 m and depth 0.72 m. The sides of the flume are consisting of glass wall. Pumps were operated to lift the water from the tank under the ground to the elevated tank. There is a valve at the elevated tank and this regulates the flow of water into the main flume. Water flows through the control valve, first enters into a tank at the upstream of the flume. The upstream tank has a dimension of 2.8 m length, 1.5 m wide and 1.5 m deep and consists of couple of wooden baffles. Wooden baffles at the upstream tank helps in straightening the flow before it enters into the main channel. There is a control gate at the flume downstream to maintain the flow depth. A tank receives the water discharge at downstream. The downstream tank is connected by a drain that supplies the water from downstream tank again to the storage below the ground level. Water discharge was estimated using a rectangular notch at channel downstream. Detailed experimental setup is presented in

Table 1
Various flow conditions for the experiments.

Flow discharge, Q, m^3/s	Flow depth, y, m	Froude no.	Reynolds no.
0.0442 (Q1)	0.0987	0.455	30,740
0.0472 (*Q2)	0.1014	0.467	32,712
0.0503 (Q3)	0.1038	0.48	34,730
0.0535 (Q4)	0.1079	0.482	36,674
0.0567 (Q5)	0.1101	0.496	38,756

* Representative experiment used for turbulence analysis.

Fig. 1. During the experiment, no surplus sediment was added at the upstream of the flume. The sediment transported in the flume was the bed material from the channel bed, that is, the experiments were conducted only under bed load transport condition. The various experimental conditions are mentioned in Table 1.

The slope of the flume is maintained at 0.0017. Bed material consists of uniform sand having D_{50} = 1.1 mm and standard deviation 1.17. The sand layer of the specified D_{50} was 21 cm thick. A test reach of 5 m is considered for the measurement. The test reach was considered at 5 m from the downstream point of the channel as shown in the Fig. 1. The mining pit of 10 cm deep was excavated in dry bed condition at 7.5 m from the downstream end of the laboratory flume. The shape and size of a pit is shown in Fig. 2.

The instantaneous velocity measurements were done using a three-beam acoustic Doppler velocimeter, (16 MHz micro ADV developed by Sontek). It works with 16 MHz acoustic frequency and it has a sampling frequency up to 50 Hz. The instrument works under cylindrical sampling volume of less than 1 cm^3. The sampling volume positioned at a distance 5 cm beneath the transducer at center. The duration of data acquisition at every depth was 3 min. Data was acquired along the longitudinal axis of the flume at 4 different locations. The position of data acquisition is presented in Fig. 3. At every section, data was collected at various flow depths. Here, Section A was at upstream and Section D was at downstream end of the pit.

The signal to noise ratio for the entire experiments was fixed at 15 and the signal correlation was kept 70% as cut off value. The correlation was decreased to 65% near the bed (Deshpande and Kumar, 2016). The ADV data included spikes and were needed to be done post processing. Acceleration threshold technique (Goring and Nikora, 2002) was applied for despiking the raw data. Threshold values of 1–1.5 were used based on hit and trial method so that, the velocity power spectra in the inertial sub-range satisfactorily fit with Kolmogorov "−5/3 law". A sample of velocity power spectrum for filtered and unfiltered data along with "Kolmogorov −5/3 law" can be obtained from Barman et al. (2018a). The uncertainty of Sontek data were checked by testing 15 samples of 180 s duration each. These samples were collected at a distance 3 mm above the bed. We found percentage uncertainty associated with mean flow velocity in longitudinal, lateral, and vertical directions are 0.66, 0.44, 0.87 respectively, and percentage uncertainty for the root mean square of velocity fluctuation in longitudinal, lateral, and vertical directions are 0.085, 0.062, 0.09 respectively.

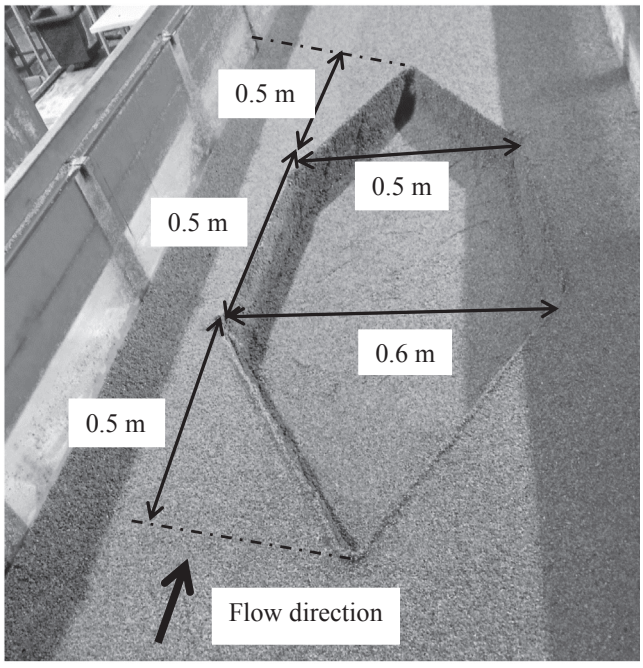

Fig. 2. Snapshot of the mining pit with dimensions.

3. Results

For investigating the turbulent flow field in a mining pit region, time-mean velocities, Reynolds shear stress, third order correlation, fourth order correlation, and turbulent kinetic energy fluxes are being analyzed in this section. The turbulent parameters are plotted against normalized depth z/h, where h = depth of flow in the section of measurement and z = distance from the channel bottom.

3.1. Time mean flow velocity and Reynolds shear stress

Time mean velocities of flow are determined from the instantaneous flow velocity using the following formula, $\bar{U} = \frac{1}{n}\sum_{i=1}^{n} u_i$; $\bar{W} = \frac{1}{n}\sum_{i=1}^{n} w_i$, where $\bar{U}$ and u_i are the time mean velocity and instantaneous velocity in longitudinal direction and $\bar{W}$ and w_i are the same in vertical direction. n is the sample numbers. Fig. 4 shows the longitudinal mean flow velocity at various section. Velocity in the mining pit gets dropped because of abrupt increase in the depth of flow. The first observation from the velocity profile is that at Section B there is negative bottom velocity up to $z/h \sim 0.3$. However, at Section C negative bottom velocity almost recovers with very small magnitude of it at channel bottom and negative velocity fully recovers at Section D. The velocity distributions are observed to be similar to that of Alfrink and van Rijn (1983), and Barman et al. (2018a) experimental results. Barman et al. (2018a) also observed reversal velocity at the bottom in the center of a symmetrical pit. From the velocity profile of earlier investigation and this research, we can conclude that recirculation zone is prominent till the center of the pit and creates a stream line separation in the central region of the pit (Alfrink and van Rijn, 1983; Barman et al., 2018a). The center for the irregular pit in this paper is referred as the center of the longitudinal axis of the pit. The flow velocity in the recirculation zone is however, smaller than the mean flow velocity near the surface. It is also noticed that the mean flow velocity near to the bed ($z/h \sim 0.04$) decreases by 29.7% at downstream Section D, comparing the upstream Section A. The flow velocity near the surface (5 cm below the free surface) also gets affected by the mining pit and it is lower than Section A by 14.9%, 41.6%, and 34.8% respectively at Section B, C, and D.

Reynolds shear stress τ_{uw} can be estimated from:

$$\left.\begin{aligned} \tau_{uw} &= -\rho_w \overline{u'w'} \\ \overline{u'w'} &= \frac{1}{n}\sum_{i=1}^{n}(u_i - \bar{U})(w_i - \bar{W}) \end{aligned}\right\}$$

. Here, u' and w' are the velocity fluctuations in longitudinal and vertical direction respectively. ρ_w represents the density of water.

Fig. 5 shows vertical profile of constant density Reynolds shear stress (RSS) distribution along with zero pressure gradient line. RSS distribution shows an increase in shear stress from the surface and reaches the maximum value, and then the stresses start to decay towards the bed surface. The decaying of shear stress towards the bed surface is called damping of RSS. Damping is caused by the reduction of

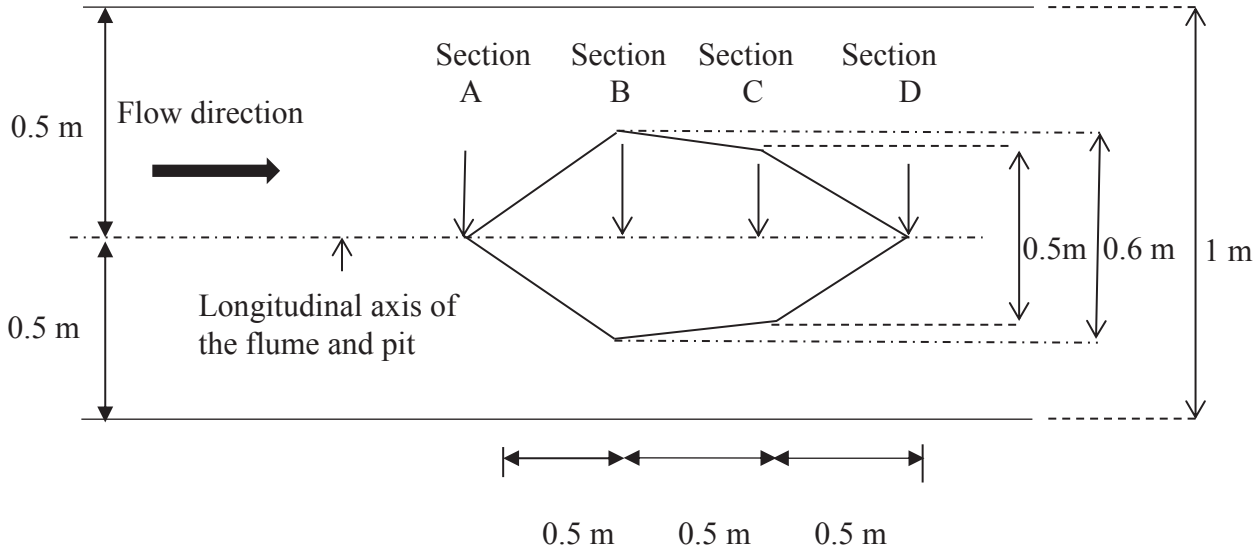

Fig. 3. location of data ADV data collection.

the relative flow velocity with respect to the particle velocity in a mobile bed (Zrostlík et al., 2016). Barman et al. (2018a) also observed similar distribution of RSS in a mining pit. Linear projection of RSS profile (zero pressure gradient) is done for calculating the shear velocity on bed using $U_* = (-\overline{u'w'})^{0.5}$ at $z = 0$ (Nezu, 1977) and is shown in Table 2. We have observed higher values of shear velocity in the pit region than the upstream section.

Table 2 shows shear velocities at different section of the test reach and shear velocity at each section are higher than the threshold shear velocity of the bed material, $u_{*c} = 0.0262$ m/s, calculated from Paphitis (2001) mean threshold curve. The critical threshold shear velocity of the bed material is also checked by Chien and Wan (1983), Hager and Oliveto (2002), and Sheppard and Renna (2005), but we have considered Paphitis (2001) for being more appropriate (Beheshti and Ataie-Ashtiani, 2008). The higher values of shear velocity represent mobile nature of the bed sediment in a channel. So, the mobility of bed particle is more in the pit and downstream end of it than upstream section as we have observed higher bed shear stress at those sections.

3.2. Higher order moment distribution of velocity fluctuations

Third order correlation means the non-symmetric distribution of velocity fluctuations. It represents the information regarding the fluxes of turbulent stresses. Zero skewness specifies the symmetric distribution

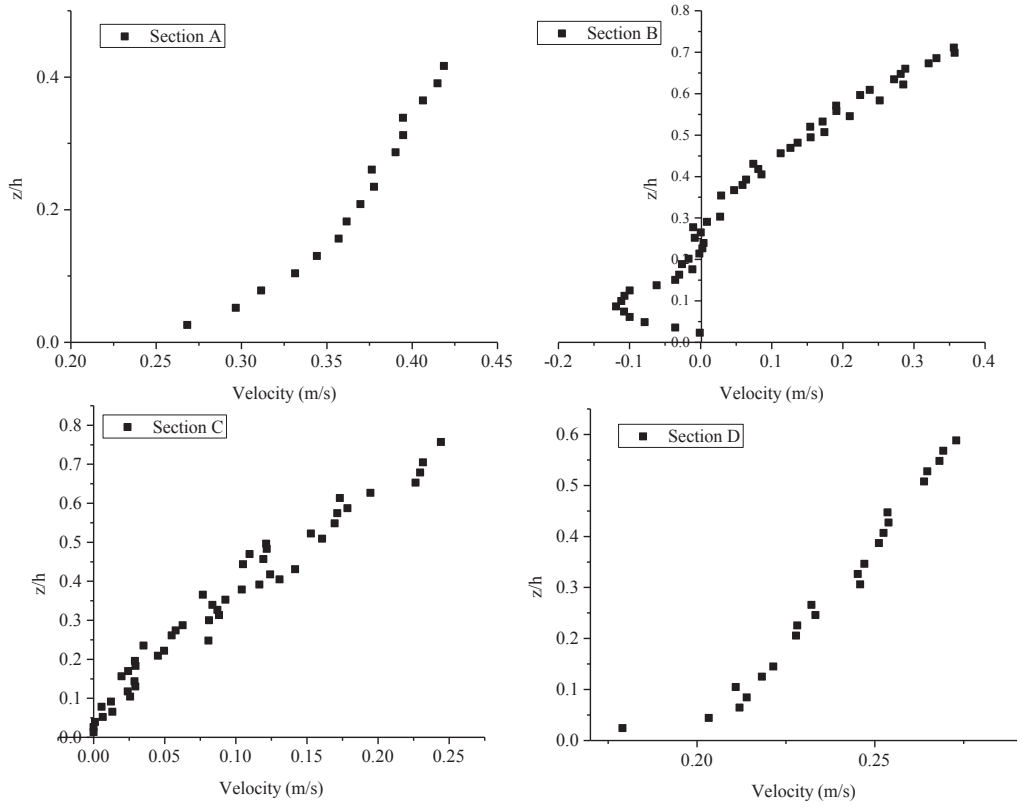

Fig. 4. stream-wise mean flow velocity at different section.

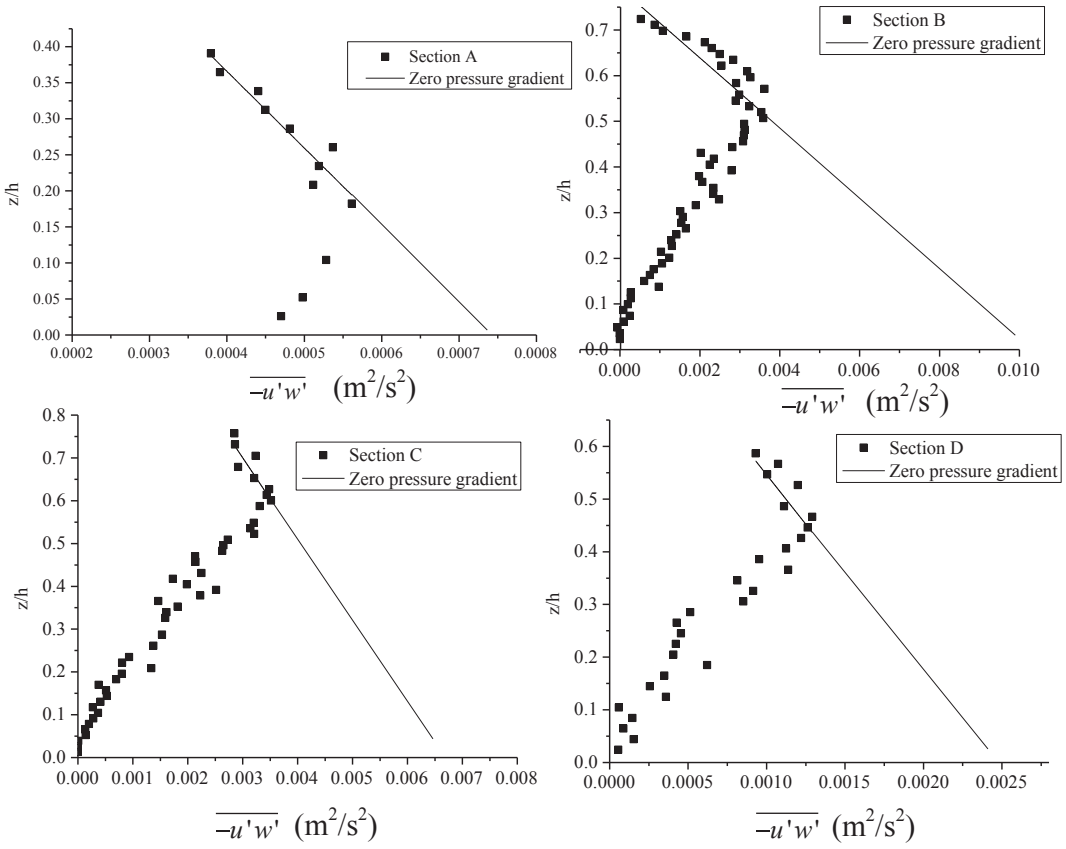

Fig. 5. Vertical distribution of Reynolds shear stress and zero pressure gradient.

Table 2
Shear velocity using RSS profile.

	Section A	Section B	Section C	Section D
U_*(m/s)	0.0273	0.1037	0.0812	0.0506

or Gaussian distribution while positive and negative skewness represent that the distribution is skewed towards right and left. The time-averaged third order moment of velocity fluctuation can be represented as (Sharma and Kumar, 2017)

$$M_{jk} = \hat{u}^j \hat{w}^k \quad \text{where } j + k = 3 \tag{1}$$

$$\hat{u} = \frac{u'}{(\overline{u'u'})^{0.5}}, \quad \hat{w} = \frac{w'}{(\overline{w'w'})^{0.5}} M_{30} = \bar{\hat{u}}^3, \quad M_{03} = \bar{\hat{u}}^3 \quad \text{where } M_{30} = \text{flux of}$$

$$M_{12} = \hat{u}\bar{\hat{w}}^2, \quad M_{21} = \hat{w}\bar{\hat{u}}^2$$

longitudinal Reynolds normal stress (RNS) in flow direction, M_{03} = vertical flux of Reynolds normal stress (RNS) in vertical to the flow direction, M_{12} = flux of vertical Reynolds normal stress (RNS) in flow direction, M_{21} = longitudinal flux of Reynolds normal stress in vertical to the flow direction.

Fig. 6(a)–(d) represents vertical profile of third order moment in four different sections of a mining pit. It is observed in Fig. 6(a) and (b) that for all the Sections, near the boundary, M_{30} begins with small positive value and M_{03} begins with small negative value. A powerful mixing flow due to the exchange of momentum near the bed surface shows Gaussian distribution of velocity fluctuation with a skewness approaching to zero. Magnitude of the positive M_{30} close to the bed is increased in the pit and downstream of it (Section B–D). The increase in positive value of longitudinal flux of longitudinal RNS suggests a strong influence on increased roughness characteristics and increased bed sediment mobility (Deshpande and Kumar, 2016) in the pit and it's downstream. The dominance of positive M_{30} rises from $z/h \approx 0.1$in upstream section to $z/h \approx 0.5 - 0.6$ in Section B and C and dominate the entire inner and outer flow region in Section D. Vertical distribution of M_{12} also follows the similar trend and shows an increase in advection of vertical RNS in flow direction in the pit and downstream of it. The higher magnitudes of positive M_{30} and M_{12} show an escalation of turbulent activities in the pit region. Again, the higher value of negative M_{03} in Section B, Section C, and Section D than Section A in the near bed region shows an increase in vertical flux of vertical RNS. The increase in dominance of M_{21} also shows the increase in advection of stream wise RNS in downward direction. The negative trend of M_{03} and M_{21}represent mobile-bed flow condition and higher bed load transport (Hanmaiahgari et al., 2017). The third order moment also identifies the effective response of the bursting events (Nezu and Nakagawa, 1993). It is understandable from Fig. 6 that positive and negative values of $M_{30}$and M_{03} near the bed surface implies sweep events in all four sections. The influence of ejection events makes M_{30} to be negative and $M_{03}$to be positive for the flow depth away from the near bed region. In this research we have observed positive M_{30} and negative M_{03} dominate till $z/h \approx 0.5 - 0.6$ in Section B, Section C, and the entire inner and outer layer of flow in Section D. This rise in dominance of positive M_{30} and negative M_{03} along the flow depth in Section B, Section C, and Section D, compared to upstream section corresponds to an increase in influence of sweep event in the pit and it's downstream. Sweep event represent high speed fluid parcel towards the bed and are mainly responsible for bed mobility. The earlier investigation by Barman et al. (2018a) also observed an increase in thickness of sweep dominance zone in the pit and it's downstream. Therefore, it is clear from the present results that the increased contribution of positive M_{30} and negative M_{03} in the pit region demonstrate a higher interchange of momentum between the flow and bed sediment particles. This momentum exchange eventually increases the sediment mobility in the pit region.

Fourth order correlation of velocity fluctuations is known as kurtosis. Turbulence intermittency can be represented by the kurtosis

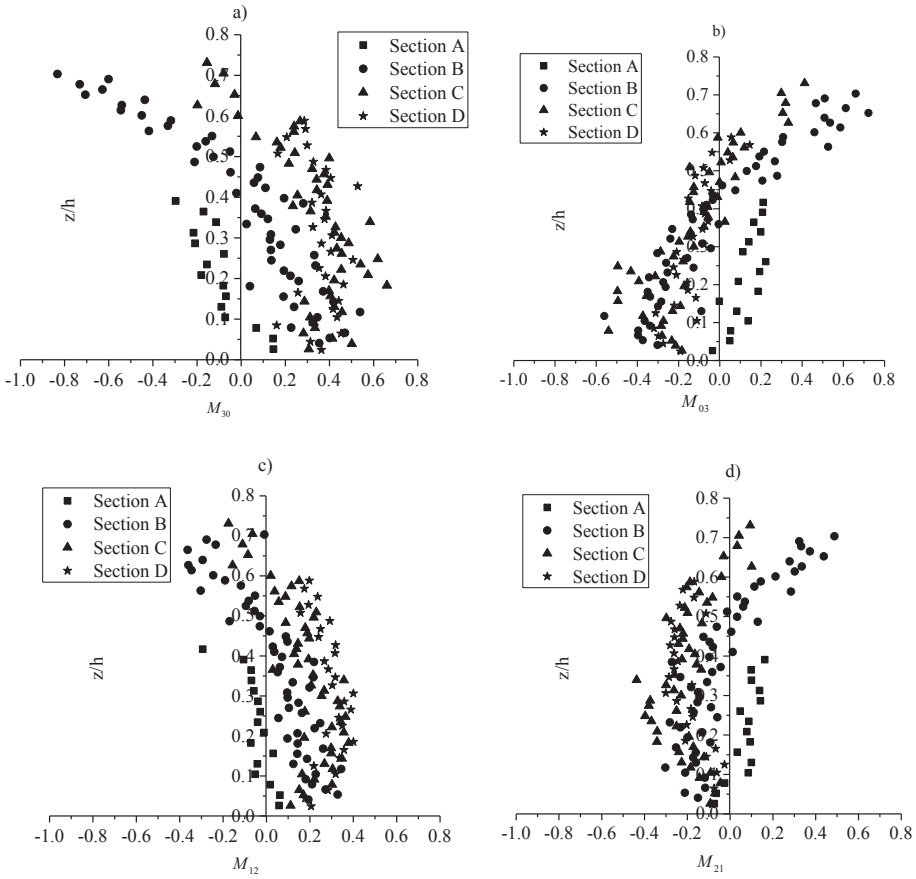

Fig. 6. Vertical distributions of third order correlation in four different section for a)M_{30}, b)M_{03}, c)M_{12}, and d) M_{21}

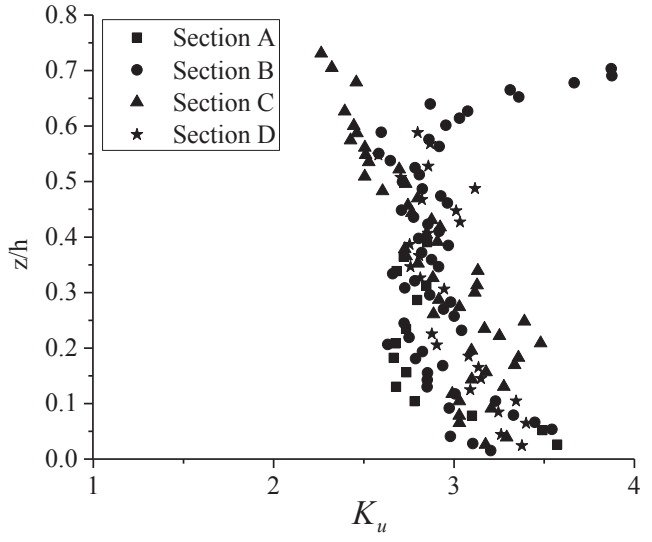

Fig. 7. kurtosis distributions at various sections

distribution. Fig. 7 shows vertical distribution of non-dimensional kurtosis $K_u = \bar{u}^4/RMS^4$ at various sections of the mining pit. Earlier literature mentioned that $K_u > 3$ shows strong characteristics and $K_u < 3$ indicates flat characteristics of turbulence intermittency (Sharma and Kumar, 2017). At Section A kurtosis shows its minimum value at $z/h \approx 0.18$ and increases both towards surface and near bed region. Maximum value of kurtosis is observed near to the bed for all other sections except Section B, which confirm highly intermittent nature of turbulence in the near bed region. Minimum kurtosis for Section B occurs at $z/h \sim 0.58$, and increases towards both outer and inner layer of flow. At Section B, we have observed maximum values of kurtosis in the outer layer (at $z/h \approx 0.7$, kurtosis = 3.87), which indicates strong intermittency in outer layer. At Section C and Section D, minimum value occurs at the outer surface and increases towards bed surface. The thickness of layer of flow dominating $K_u > 3$ rises from $z/h \approx 0.08$ in Section A to $z/h \approx 0.12$ in Section B, $z/h \approx 0.34$ in Section C, and further $z/h \approx 0.48$ in Section D, indicating higher turbulent intermittency in the mining pit region as compared to Section A.

3.3. Turbulent kinetic energy fluxes

Turbulent kinetic energy (TKE) in flow and vertical to the flow directions for two dimensional analyses is $f_{ku} = 0.75(\bar{u'^3} + \bar{u'w'^2})$ and $f_{kw} = 0.75(\bar{w'^3} + \bar{w'u'^2})$ respectively (Sharma and Kumar, 2017). The TKE can be normalized by using $F_{ku} = f_{ku}/U_*^3$ and $F_{kw} = f_{kw}/U_*^3$ and is presented in Fig. 8.

The transport of TKE occurs from the zone of high energy to the low energy. For all four sections $F_{ku}$is positive and F_{kw} is negative near the boundary. The positive F_{ku}implies longitudinal TKE flux in flow direction while, negative F_{kw} represents the vertical TKE flux in the downward direction. Mobility of bed particles are caused by positive F_{ku} and negative F_{kw}. Fig. 8 clearly shows positive F_{ku} changes to negative F_{ku} at $z/h \approx 0.1$ in Section A, while it changes to negative at $z/h \approx 0.5 - 0.6$ in Section B and Section C. At Section D positive F_{ku}remains positive throughout flow depth. Similar trend is observed in the vertical distribution of vertical TKE flux, where F_{kw} changes from negative to positive moving away from bed. It is noted that the dominance of positive $F_{ku}$and negative F_{kw} increases in the mining pit region, which can increase bed particle mobility in that region. Again, analyzing the magnitude of TKE fluxes in all four sections from Fig. 8, the reduction in the

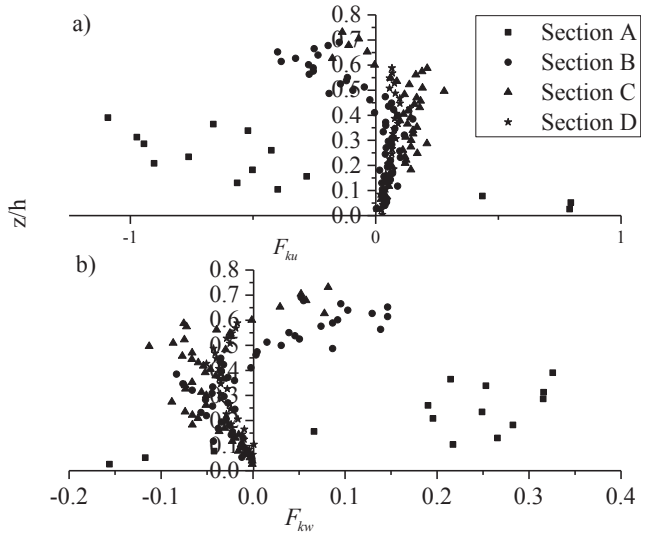

Fig. 8. Vertical distributions of normalized TKE flux a) stream-wise direction and b) vertical to the stream-wise direction

magnitude of normalized TKE fluxes in Section B, Section C, and Section D is due to higher values of normalizing factor U_* as compared to the upstream section (Section A). We have found 3.14 times increase in longitudinal TKE flux and 5.8 times increase in vertical TKE flux at $z/h \sim 0.05$ in Section B and 1.14 times increase in longitudinal TKE flux in Section C as compared to Section A. There is also a reduction in longitudinal TKE flux in Section D by 4.11 times, and vertical TKE flux in section C and Section D by 1.3 times and 11.8 times respectively at $z/h \approx 0.05$. It is also clear from the analysis of TKE that in Section B to Section D, positive $F_{ku}$and negative F_{kw} increases along the flow depth from the bed surface and reaches maximum value at $z/h \approx 0.4 - 0.5$, and changes its sign at $z/h \approx 0.5 - 0.6$ in Section B and Section C. At Section D, there is positive $F_{ku}$and negative F_{kw} for entire z/h. The results from TKE fluxes show that, TKE fluxes are transported in downstream and downward direction in the both turbulent inner layer ($z/h \leqslant 0.2$) and outer layer ($z/h > 0.2$) of the mining pit.

3.4. Bed load transport prediction for various shaped mining pit

Disturbance in the channel bed causes change in mobility of the bed particles. Kondolf (1997) observed increase in sediment transport rate in a channel underwent aggregate mining. Barman et al. (2018b) also shows more bed load transport rate for a channel with mining pit than the plain bed channel. In the present experiment bed load discharge was collected in a bed load collection tank positioned at channel downstream. The mining pit in the channel also acts as a sediment entrapper, which collects the sediment transported from the pit upstream and thus the migration of upstream edge occurs. The erosion at the downstream of the pit has been observed higher than the upstream and has been discussed by Barman et al. (2018a). Barman et al. (2018a) developed a bed load prediction equation by considering bed load discharge only as a function of flow velocity and bed sediment characteristics. In this investigation, the bed load transport equation developed by Barman et al. (2018a) is modified using a correction factor for various shape of mining pit. A shape factor based on length to width ratio of the mining pit is applied as correction factor to the earlier developed equation. Bed load discharge data for mining pit with length to width ratio 0.82, 1.025, 2, and 2.5 for bed material of $D_{50} = 1.1$ mm and 0.418 mm at various discharge as mentioned in Table 1 are used for modifying the earlier developed bed load transport equation. The depth of the pit was kept constant for all shape of the pit. The earlier developed bed load transport formulation is given by Eq. (2)

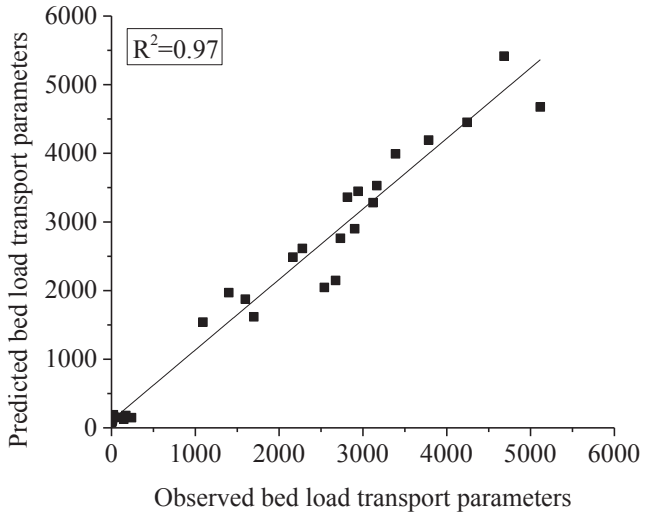

Fig. 9. Predicted bed load transport parameters

$$q_b = 1.873e^{0.237\frac{u-u_{*c}}{u_{*c}}} \tag{2}$$

where $q_b = \frac{Q_b}{(\rho_s - \rho)\nu d_{50}}$ = dimensionless bed load transport parameter, Q_b is the bed load discharge rate in kg/s, ρ, ρ_s and $\nu$are the density of water, bed material, and kinematic viscosity of water, $u = Q/y$ is average flow velocity, Qrepresents flow discharge, $y$is the depth of flow, $u_{*c}$is the threshold shear velocity of bed sediment. Eq. (2) is modified introducing a correction factor based on maximum length and width of a mining pit. The consolidated form of the modified bed load transport formula is as follows

$$q_b = 1.873\left(\frac{L}{B}\right)^{0.22} e^{0.237\frac{u-u_{*c}}{u_{*c}}} \tag{3}$$

where, L is the maximum length of the pit, B is the maximum width of the pit. The predicted bed load transport rate corresponds to the experimental value are presented in Fig. 9.

Sensitivity analysis of presently developed bedload transport equation is carried out to understand the influence of flow velocity (u), critical shear velocity (u_{*c}) and pit geometry (L/B) on bedload transport. It is observed from the Fig. 10 that bed load discharge is highly sensitive to the flow and sediment property and comparatively less sensitive to pit geometry.

The present study shows an increase in turbulence in the mining zone that subsequently increases the erosion of the channel bed. It

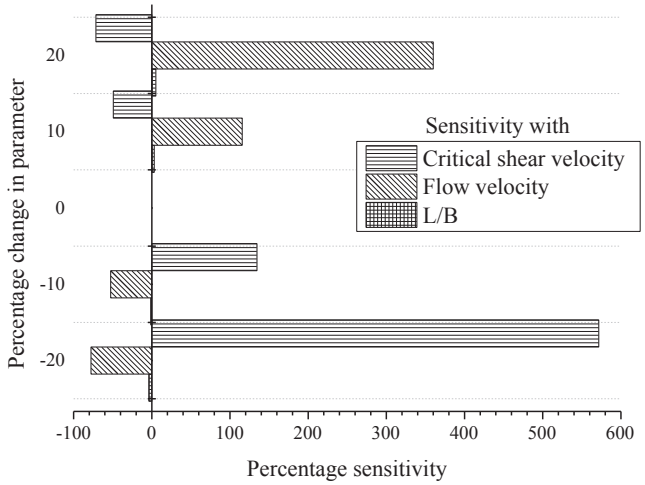

Fig. 10. Sensitivity bedload transport with respect to pit geometry (L/B), flow velocity and critical shear velocity

shows a variation of hydrodynamic characteristics in the pit region that affects the morphology and bedload transport of the channel. Water flowing with high velocity over an excavated bed can cause high scouring that increases electric conductivity and hardness of the water (Erskine, 1990). It also causes adverse effects on the species attached to streambed deposits and flora and fauna of the river basin (Padmalal et al., 2008). The anthropogenic disturbance such as sand mining and complex interaction of flow with channel morphology necessitates the needs for rigorous water quality sampling (Gomes and Wai, 2014) and also increases the cost of downstream water treatment (Kim, 2005). The morphological processes of channel bed are important for aquatic habitat (Newson and Newson, 2000). Mining pit becomes a distinct morphological features like pools, run, and riffles of a river, thus it can acts as mesoscale physical habitats that farther improve the habitat assessment. The mesohabitat structures of pool and riffle are important factors that shows the biological integrity and ecological stream health of a river (Calderon and An, 2016). The present research can be applied for giving a detail of change in flow and sediment transport characteristics in a mining location, which further affects the ecology of a river.

4. Conclusions

Flow characteristics in a sand mining pit are studied based on experimental data. An irregular mining pit is considered and effects of the pit on various turbulent parameters like velocity profile, RSS, higher order moments, and turbulent kinetic energy fluxes are discussed. Velocity profile shows reversal bottom velocity at Section B which is 0.25 m upstream from the center of the pit. The negative bottom velocity gets recovered at Section C, 0.25 m downstream from the center of the mining pit. Longitudinal velocity distributions suggest separation of stream line at the center of the mining pit. Reynolds shear stress shows an increase in maximum values of shear stress at Section B, C, and D while comparing with Section A. RSS distribution also shows and increase in damping of RSS in the pit. Zero pressure gradient of RSS distribution shows 3.8, 2.97, and 1.85 times higher values of total bed shear velocity at Section B, C, and D than Section A. Near the bed, greater positive values of M_{30} and greater negative values of M_{03} in Section B to Section D than those of Section A shows strong influence on increased roughness characteristics and increased bed particle mobility. The distribution of M_{30} and M_{03} also explain the occurrence of various bursting events in the flow. This increase in dominance of positive M_{30} and negative M_{03} till $z/h \sim 0.5 - 0.6$ in Section B, Section C, and the entire inner and outer flow layer in Section D corresponds to an increase in influence of sweep event in the pit and downstream of it than the upstream section. The Kurtosis distribution shows that the thickness of layer of flow dominating $K_u > 3$ rises from $z/h \sim 0.08$ in Section A to $z/h \sim 0.12$ in Section B, $z/h \sim 0.34$ in Section C, and further $z/h \sim 0.48$ in Section D, correspond a higher turbulent intermittency in the pit region than upstream section. The experimental results show an increase in dominance of positive $F_{ku}$and negative F_{kw} in the mining pit region, suggest an increased flux of TKE which can be correlated to the increased bed particle mobility in that region. The analysis of TKE shows that in Section B to Section D, TKE fluxes are transported in downstream and downward direction in the turbulent inner layer ($z/h \leqslant 0.2$) and outer layer ($z/h > 0.2$), while it is in upstream and upward direction in Section A for $z/h > 0.1$. The studies on various turbulent parameters of flow show the change in these parameters due to the disturbance in the channel bed, which can further affect the channel morphology. We have also modified an earlier developed bed load transport equation by introducing a shape factor (length to width ratio) based on various dimension of the mining pit. Consideration of bed sediment transport as a function of pit dimension enables us to apply the modified equation in a channel having irregular mining pit. However, the bed load transport equation is associated with the experimental limitation and can be further enhance using data from an actual river.

Appendix A. Supplementary data

Supplementary data to this article can be found online at https://doi.org/10.1016/j.ecoleng.2019.05.013.

References

Alfrink, B.J., Van Rijn, L.C., 1983. Two- Equation turbulence model for flow in Trenches. J. Prof. Issues Eng. 109 (3), 941–958.

Barman, B., Sharma, A., Kumar, B., Sarma, A.K., 2017. Multiscale characterization of Migrating Sand Wave in Mining Induced Alluvial channel. Ecol. Eng. 102, 199–206.

Barman, B., Kumar, B., Sarma, A.K., 2018a. Turbulent flow structures and geomorphic characteristics of mining affected alluvial channel. Earth Surf. Proc. Land. 43 (9), 1811–1824.

Barman, B., Kumar, B., Sarma, A.K., 2018b. Dynamic characterization of the migration of a mining pit in an alluvial channel. Int. J. Sediment Res. https://doi.org/10.1016/j.ijsrc.2018.10.009.

Beheshti, A.A., Ataie-Ashtiani, B., 2008. Analysis of threshold and incipient conditions for sediment movement. Coast. Eng. 55, 423–430.

Bennett, S.J., Bridge, J.S., 1995. The geometry and dynamics of low-relief bed forms in heterogeneous sediment in a laboratory channel, and their relationship to water flow and sediment transport. J. Sediment Res. A65, 29–39.

Best, J., 1992. On the entrainment of sediment and initiation of bed defects: insights from recent developments within turbulent boundary layer research. Sedimentology 39 (5), 797–811.

Brestolani, F., Solari, L., Rinaldi, M., Lollino, G., 2015. On morphological impacts of gravel mining: the case of the Orco River. Eng. Geol. Soc. Teritory 3, 319–322.

Calderon, M.S., An, K.G., 2016. An influence of mesohabitat structures (pool, riffle, and run) and land-use pattern on the index of biological integrity in the Geum River watershed. J. Ecol. Environ. 40, 13. https://doi.org/10.1186/s41610-016-0018-8.

Calle, M., Alho, P., Benito, G., 2017. Channel dynamics and geomorphic resilience in an ephemeral Mediterranean river affected by gravel mining. Geomorphology 285, 333–346.

Cao, Z., 1997. Turbulent bursting-based sediment entrainment function. J. Hydraul. Eng. 123 (3), 233–236.

Chen D, Liu M. 2009. One- and Two-dimensional modelling of deep gravel mining in the Rio Salado. World Environmental and Water Resources Congress pp. 3462-3470.

Chien, N., Wan, Z.H., 1983. Mechanics of Sediment Movement. Science Publications, Beijing (in Chinese).

Clifford, N.J., McClatchey, J., French, J.R., 1991. Measurements of turbulence in the benthic boundary layer over a gravel bed and comparison between acoustic measurements and predictions of the bedload transport of marine gravels. Sedimentology 38 (1), 161–171.

Collins, B.D., Dunne, T., 1989. Gravel transport, gravel harvesting, and channel bed degradation in rivers draining the Southern Olympic Mountains, Washington, U.S.A. Environ. Geol. 13, 213–224.

Collins BD, Dunne T, 1990. Fluvial geomorphology and river gravel mining: a guide for planners. California division of mines and geology, special publication 98, Sacramento, CA.

Deshpande, V., Kumar, B., 2016. Turbulent flow structures in alluvial channels with curved cross-sections under conditions of downward seepage. Earth Surf. Proc. Land. 41, 1073–1087.

Drake, T.G., Shreve, R.L., Dietrich, W.E., Whiting, P.J., Leopold, L.B., 1988. Bedload transport of fine gravel observed by motion picture photography. J. Fluid Mech. 192, 193–217.

Dwivedi, A., Melville, B., Shamseldin, A.Y., 2010. Hydrodynamic forces generated on a spherical sediment particle during entrainment. J. Hydraul. Eng. 136 (10), 756–769.

Erskine, W.D., 1990. Environmental impacts of sand and gravel extraction on river systems. In: The Brisbane River: A Source Book for the Future. Australian Littoral Society, Moorooka, pp. 295–302.

Gomes, P.I.A., Wai, O.W.H., 2014. Sampling at mesoscale physical habitats to explain headwater stream water quality variations: its comparison to equal-spaced sampling under seasonal and rainfall aided flushing states. J. Hydrol. 519, 3615–3633.

Goring, D.G., Nikora, V.I., 2002. Despiking acoustic doppler velocimeter data. J. Hydraul. Eng. 128 (1), 117–126.

Hager, W.H., Oliveto, G., 2002. Shields' entrainment criterion in bridge hydraulics. J. Hydraul. Eng. 128 (5), 538–542.

Hanmaiahgari, P.R., Roussinova, V., Balachandar, R., 2017. Turbulence characteristics of flow in an open channel with temporally varying mobile bedforms. J. Hydrol. Hydromech. 65 (1), 35–48.

Kim, C., 2005. Impact analysis of river aggregate mining on river environment. KSCE J. Civ. Eng. 9, 45–48.

Kline, S.J., Reynolds, W.C., Schraub, F.A., Runstadler, P.W., 1967. The structure of turbulent boundary layers. J. Fluid Mech. 30, 741–773.

Kondolf, G.M., 1997. Hungry water: effects of dams and gravel mining on river channels. Environ. Manage. 21 (4), 533–551.

Lee, H.Y., Fu, D.T., Song, M.H., 1993. Migration of rectangular mining pit composed of uniform sediment. J. Hydraul. Eng. 119, 64–80.

Nelson, J.M., Shreve, R.L., McLean, S.R., Drake, T.G., 1995. Role of near-bed turbulence structure in bed load transport and bed form mechanics. Water Resour. Res. 31 (8), 2071–2086.

Newson, M.D., Newson, C.L., 2000. Geomorphology, ecology and river channel habitat; mesoscale approaches to basin-scale challenges. Prog. Phys. Geogr. 24 (2), 195–217.
Neyshabouri, S.A.A.S., Farhadzadeh, A., Amini, A., 2002. Experimental and field study of mining pit migration. Int. J. Sedim. Res. 17 (4), 323–333.
Nezu, I., Nakagawa, H., 1993. Turbulence in open channels. IAHR/AIRH Monograph. Balkema, Rotterdam, The Netherlands.
Nezu, I., 1977. Turbulent Structure in Open Channel Flow. PhD thesis. Kyoto University, Kyoto, Japan).
Nikora, V., Goring, D., 2000. Flow turbulence over fixed and weakly mobile gravel beds. J. Hydraul. Eng. 126 (9), 679–690.
Padmalal, D., Maya, K., Sreebha, S., Sreeja, R., 2008. Environmental effects of river sand mining: a case from the river catchments of Vembanad lake, Southwest coast of India. Environ. Geol. 54 (4), 879–889.
Paphitis, D., 2001. Sediment movement under unidirectional flows: an assessment of empirical threshold curves. Coast. Eng. 43, 227–245.
Ramkumar, M., Kumaraswamy, K., James, R.A., Suresh, M., Sugantha, T., Jayaraj, L., Mathiyalagan, A., Saraswathi, M., Shyamala, J., 2015. Sand mining, channel bar dynamics and sediment textural properties of the Kaveri river, South India: implications on flooding hazard and sustainability of the natural fluvial system. Environ. Manage. River Basin Ecosyst. https://doi.org/10.1007/978-3-319-13425-3_14: 283-318.
Rinaldi, M., Wyżga, B., Surian, N., 2005. Sediment mining in alluvial channels: physical effects and management perspective. River Res. Appl. 21, 805–828.
Sear, D.A., Archer, D., 1998. Effects of gravel extraction on stability of gravel-bed rivers: the Wooler Water, Northumberland, UK. Water Resources Publications, Highlands Ranch, Colo, pp. 415–432.
Sharma, A., Kumar, B., 2017. Structure of turbulence over non uniform sand bed channel with downward seepage. Eur. J. Mech.-B/Fluids 65, 530–551.
Sheppard, D.M., Renna, R., 2005. Florida Bridge Scour Manual. Florida Department of Transportation, Tallahassee, FL, 605 Suwannee Street 32399-0450.
Song, T., Graf, W.H., 1994. Non-uniform open-channel flow over a rough bed. J. Hydrosci. Hydraul. Eng. Tokyo 12 (1), 1–25.
Sutherland, A.J., 1967. Proposed mechanism for sediment entrainment by turbulent flows. J. Geophys. Res. 72, 6183–6194.
Thorne, P.D., Williams, J.J., Heathershaw, A.D., 1989. In situ acoustic measurements of marine gravel threshold and transport. Sedimentology 36 (1), 61–74.
Venditti, J.G., Church, M.A., Bennett, S.J., 2005. Bed form initiation from a flat sand bed. J. Geophys. Res. 110, F01009.
Yuill, B.T., Gaweesh, A., Allison, M.A., Meselhe, E.A., 2016. Morphodynamic evolution of a lower Mississippi River channel bar after sand mining. Earth Surf. Proc. Land. 41 (4), 526–542.
Zawiejska, J., Wyżga, B., Pawlik, A.R., 2015. Variation of bed material along mountain river modified by gravel extraction and channelization, the Czarny Dunajec, Polish Carpathians. Geomorphology 231, 353–366.
Zrostlík, Š., Bareš, V., Krupička, J., Picek, T., Matoušek, V., 2016. Distribution of velocity and turbulent characteristics in coarse-sediment laden flows above erodible plane bed in open channel. EPJ. Web Conf. 114, 02144.